ARCHIVES OF ELECTRICAL ENGINEERING VOL. 68(4), pp. 891–905 (2019)

DOI 10.24425/aee.2019.130690

Averaged model of a buck DC–DC converter for single-loop description of current-mode control

Włodzimierz Janke, Maciej Bączek, Jarosław Kraśniewski

Department of Electronics and Computer Science
Koszalin University of Technology
Śniadeckich Street 2, 75-453 Koszalin, Poland
e-mail: jaroslaw.krasniewski@ie.tu.koszalin.pl

(Received: 30.04.2019, revised: 15.07.2019)

Abstract: Averaged models: an AC large signal, DC and AC small signals of a current-controlled buck converter are described. Only peak current mode control of a converter working in the continuous conduction mode (CCM) is considered. The model derivation differs from the typical approaches presented in the literature and doesn't refer to the multi-loop concept of a current controlled converter. The separation of the variables method is used in the model derivation. The resulting models are presented in the form of an equation set and equivalent circuits. The calculations based on the presented models are verified by measurements and full-wave PSpice simulations.

Key words: averaged model, buck converter, continuous conduction mode, peak current mode control

1. Introduction

A buck converter, also known as a step-down converter is one of the most popular DC-DC switch-mode power converters. Averaged models are usually used for the description of the converter behavior for time scales containing many switching periods (in other words: in the low frequency range). Such models are necessary in the process of designing control algorithms and circuits for converters [1, 2]. The current-mode control (CMC) is one of the possible control schemes and is widely discussed in many papers, technical notes and textbooks, where, among others, the advantages of CMC over voltage-mode control (VMC) are pointed out. Several versions of current mode control are known, such as peak current mode control (PCMC), average current mode control, valley current mode control and others. Only PCMC for a buck converter in a continuous conduction mode (CCM) is discussed in the further text.

It is well-known that in a standard VMC, the main switch in the power stage of a converter (being switched *ON* at the beginning of the switching period) is switched *OFF* at the moment t_{ON} and the time t_{ON} (or the duty ratio $d_A = t_{ON}/T_S$, where T_S is a switching period) is the output signal of the control circuit. In the CMC (in PCMC variant), the main switch is switched *OFF* when the instantaneous value of the rising inductor current becomes equal to the value of the current i_W established by a control circuit. The principal idea of the current mode control was proposed in 1978 [3, 4] and the detailed analysis and modeling of current controlled converters has been presented in 1979 [5] and next in many further papers, among others in the comprehensive studies of Middlebrook [6, 7] published in 1985 and 1989 respectively. One of the specific features of current-controlled converters observed in the early analyses is the instability of a converter in the case if the duty ratio of a switching signal exceeds 0.5. The solution of the instability problem is to use the additional external ramp in the control loop. This external ramp is taken into account in the description of current controlled converters presented in further publications. Averaged models of the current controlled converters described in [5, 6] and [7] are derived with the use of the state-space averaging approach. The attempts of description of a current control method within the frame of state-space averaging leads to the concept of a double (or generally – multiple) control loop (presented also by Ridley in [8]) as a characteristic feature of current-mode control, where specifically, the "inner loop" is referred to as a "current loop" and the outer – as a voltage loop. The "inner loop" describes the dependence of the inductor current on the control quantity, namely current i_W or a corresponding voltage and other circuit variables. According to [5–7], the inner control loop is responsible for the above mentioned instability. In some, variants of the discussed models, the inductor current is treated as an independent variable and the resulting model is of the first order (only one pole in the small signal averaged model, corresponding to the angular frequency $1/RC$, where R is the load resistance and C – capacitance of the capacitor connected to the converter output). Other models are usually of the second (or even higher) order.

In the next model of current controlled converters, presented by Ridley in 1991, the relatively new idea of the averaged models derivation, presented by Vorperian in 1990 [9, 10], based on the concept of a three-terminal switch model, is adopted. A similar idea of creating the averaged model of a pair of switches is adopted in the so called behavioral relationship in [11]. The derivation of averaged models of pulse-modulated converters based on a three-terminal switch model instead of the state-space averaging approach has been widely accepted and used, among others, to the current-controlled converter modeling, but the double-loop description is still present in papers based on this approach.

In papers of Ridley [12, 13] it is pointed out, that continuous-time models of current-controlled converters [5–7] cannot predict the instability of the converter, observed experimentally. This opinion is repeated in many other papers (for example [14–18]) and seems to be generally accepted. Sampled-data models have been proposed by Ridley for proper description of the instability phenomenon. The modified continuous-time models have been obtained by various approximations of the e^{sT} term in sampled-data models. Other attempts to the modeling of various variants of current-controlled converters and different variants of the analog or digital control subcircuit are presented in more modern papers, as for example in [19–22]. The newest papers in the field (as for example [23–27]) are devoted to the practical implementations of various digital techniques of current mode control and does not concern strictly the topic of averaged models.

Small-signal averaged models of current controlled converters discussed in some papers, for example [14–18], have the form of the transmittances of the fourth (or higher) order. The applicability of such complex transmittances to the design of control circuits seems to be questionable. On the other hand, models discussed in [14–18] are derived on a basis of double-loop description of current-controlled converters. It may be inferred, that the concept of a double-control loop is not a convenient way of current-controlled converter description.

The main purpose of this paper is to derive the continuous-time averaged model of a pulse modulated converter without the use of the double-loop concept. The buck converter in a continuous conduction mode (CCM) is taken as an example and the separation of the variables method [28, 29] is used in the model derivation. In this paper, the current i_W is treated as a control quantity and t_{ON} as well as duty ratio d_A are secondary variables. The connection between the control current and the inductor current is described by introducing the quantity i_X being the difference between the control current i_W and the averaged inductor current in a single switching period. The presented approach to current-controlled converter modeling may be a convenient alternative to modeling based on a double control loop approach.

An outline of the proposed method has been previously presented in the short paper [30] on the example of an ideal buck converter without small-signal analysis, and without verification of dynamic characteristics. The present paper is a substantial extension of [30], takes into account parasitic resistances of converter components and includes verification of the proposed model by measurements and full-wave simulations.

The large-signal averaged model is presented in Section 2. The DC and small-signal averaged models and the resulting transmittances are discussed in Sections 3 and 4. The numerical calculations and experiments are described in Section 5. Section 6 contains some concluding remarks.

2. Large-signal averaged model of current-controlled buck converter

The considered power stage of the converter and its equivalents for the *ON* and *OFF* subintervals are depicted in Figs. 1(a, b) and (c), respectively. The waveform of the inductor current $i_L(t)$ in a single switching period is presented in Fig. 2. According to the idea of an averaged model, each circuit variable in a given period is represented by its averaged value and these averages are varying slowly (with low frequency) in consecutive switching periods. The symbol $i_L(t)$ describing the waveform of the inductor current inside a single period should be distinguished from i_{LS} representing the average value in a given period. Symbols of other variables such as v_G (input voltage), v_O (output voltage) and i_W (control current) denote averaged values in a given period.

The changes of the current i_W forced by a control circuit influence the averaged inductor current i_{LS}. The difference:

$$i_X = i_W - i_{LS} \tag{1}$$

depends on other circuit variables and this dependence is crucial for the averaged model. From Figs. 1(b, c) and 2 one can find the dependencies of i_X on the input and output voltage and the time t_{ON}.

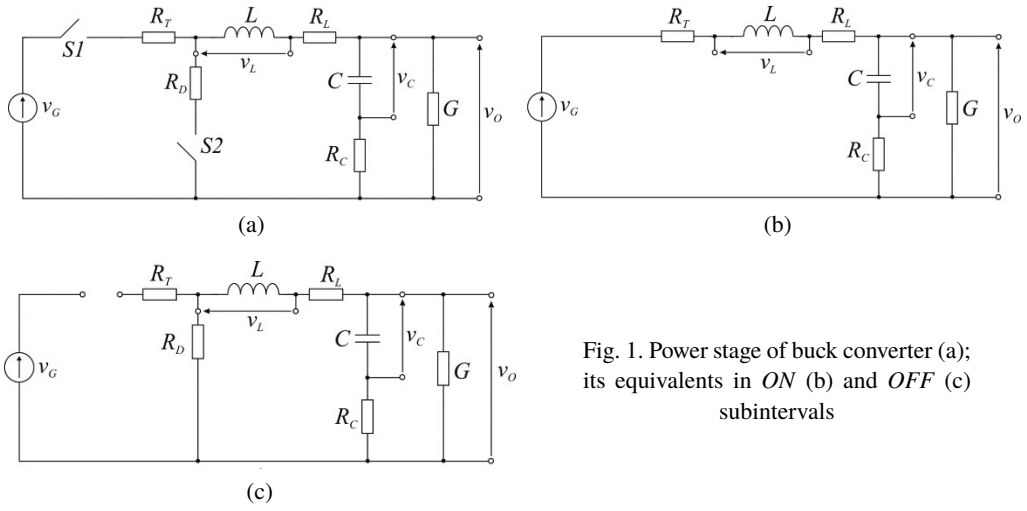

Fig. 1. Power stage of buck converter (a); its equivalents in *ON* (b) and *OFF* (c) subintervals

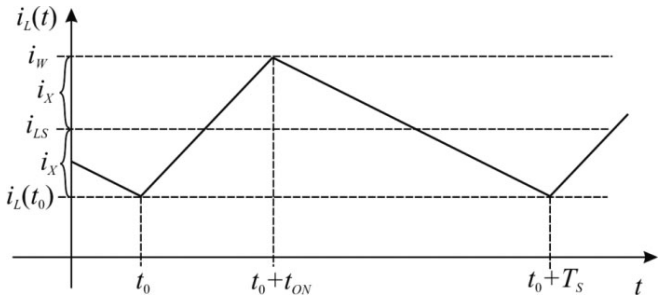

Fig. 2. The waveform of the inductor current of buck in a single switching period

From Fig. 1(b) for the *ON* subinterval:

$$i_L\,(t_0 + t_{ON}) = i_L(t_0) + \frac{1}{L}\int_{t_0}^{t_0+t_{ON}} [v_G - v_O - i_L(t)\cdot(R_T + R_L)]\cdot \mathrm{d}t. \tag{2}$$

Denoting:

$$R_1 = R_T + R_L\,, \qquad R_2 = R_D + R_L \tag{3}$$

and taking for simplicity $t_0 = 0$, one obtains:

$$i_L\,(t_{ON}) = i_L(0) + \frac{1}{L}\int_{0}^{t_{ON}} [v_G - v_O - i_L(t)\cdot R_1]\cdot \mathrm{d}t. \tag{4}$$

The term containing $i_L(t)$ under an integral is much smaller than $v_G - v_O$. Calculations may be simplified by replacing $i_L(t)$ under an integral by its average value i_{LS}. The result is:

$$i_L(t_{ON}) = i_L(0) + \frac{1}{L} \cdot (v_G - v_O - i_{LS} \cdot R_1) \cdot t_{ON}, \tag{5}$$

therefore:

$$\Delta i_L = i_L(t_{ON}) - i_L(0) = \frac{1}{L} \cdot (v_G - v_O - i_{LS} \cdot R_1) \cdot t_{ON}\,. \tag{6}$$

Similar dependence may be obtained for the *OFF* subinterval:

$$\Delta i_L = i_L(t_{ON}) - i_L(T_S) = \frac{T_S - t_{ON}}{L} \cdot (v_O + R_2 \cdot i_{LS})\,. \tag{7}$$

For a low-frequency range it may be assumed that the values of v_O during a single switching period are the same for the *ON* and *OFF* subintervals, therefore from Eqs. (6) and (7), using $d_A = t_{ON}/T_S$ one obtains:

$$d_A = \frac{v_O + i_{LS} \cdot R_2}{v_G + i_{LS} \cdot (R_2 - R_1)}\,. \tag{8}$$

In derivation of the averaged model of a switching converter with the separation of the variables approach [28, 29], all circuit variables are divided into two groups. The first contains variables having the same local averages in the *ON* and *OFF* subintervals and the second-variables having different local averages in *ON* and *OFF*. The first group in the present case contains quantities v_G, v_O, i_L, i_W and the second-quantities v_L (the voltage on the ideal part of the inductor – see Fig. 1) and i_G (the input current).

The averaged value of v_L is:

$$\begin{aligned} v_{LS} &= d_A \cdot v_L(ON) + (1 - d_A) \cdot v_L(OFF) \\ &= d_A \cdot (v_G - v_O - i_L \cdot R_1) + (1 - d_A) \cdot (-v_O - i_L \cdot R_2) \end{aligned}, \tag{9}$$

After introducing Eq. (8) into (9) one obtains:

$$v_{LS} = 0, \tag{10}$$

therefore, the ideal part of the inductor is shorted in the averaged model.

The averaged value of the input current is:

$$i_{GS} = d_A \cdot i_G(ON) + (1 - d_A) \cdot i_G(OFF) = i_{LS} \cdot d_A\,. \tag{11}$$

From Eqs. (8) and (11) we have:

$$i_{GS} = i_{LS} \cdot \frac{v_O + i_{LS} \cdot R_2}{v_G + i_{LS} \cdot (R_2 - R_1)}. \tag{12}$$

The difference i_X defined by Eq. (1) is:

$$i_X = i_W - i_{LS} = \frac{\Delta i_L}{2}. \tag{13}$$

By introducing Eq. (8) into (6), with the use of (13) one obtains:

$$i_X \approx G_Z \cdot \frac{v_O \cdot (v_G - v_O) + i_{LS} \cdot [R_2 \cdot v_G - (R_1 + R_2) \cdot v_O]}{v_G + i_{LS} \cdot (R_2 - R_1)}, \tag{14}$$

where:

$$G_Z = \frac{T_S}{2 \cdot L}. \tag{15}$$

Eq. (14) is obtained as an approximation of the exact formula. The omitted term $R_1 \cdot R_2 \cdot i_{LS}^2$ in the numerator of Eq. (14) is three to four orders smaller than the main term $v_O \cdot (v_G - v_O)$ for typical values of circuit parameters.

The additional equations describing the output cell of the converter, valid in both subintervals are:

$$v_O = v_C + R_C \cdot \frac{\mathrm{d}v_C}{\mathrm{d}t}, \tag{16}$$

$$i_L = C \cdot \frac{\mathrm{d}v_C}{\mathrm{d}t} + G \cdot v_O. \tag{17}$$

The equivalent circuit representing the large-signal model of a current-controlled buck converter in a continuous conduction mode (CCM), based on Eqs. (1), (10), (12), (14), (16), (17) is shown in Fig. 3. It differs from the model discussed in [30] by the existence of the capacitor series resistance R_C and different description of the current sources i_X and i_{GS} – see Eqs. (12) and (14).

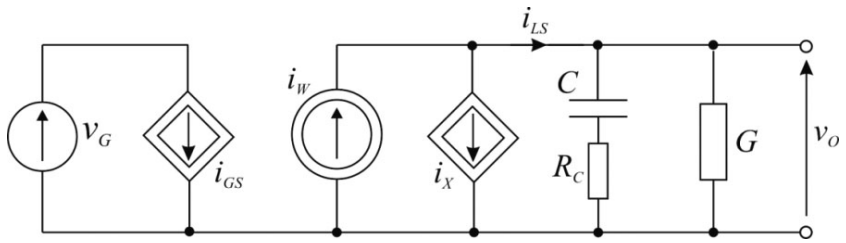

Fig. 3. The averaged large-signal model of a current-controlled buck converter in CCM

3. DC model

The DC model is obtained from the AC large-signal model by replacing the capacitor branch by an open-circuit and using symbols of DC quantities for circuit variables. The result is shown in Fig. 4. From this figure we obtain:

$$I_L = G \cdot V_O. \tag{18}$$

From Fig. 4 and DC equivalents of Eqs. (13) and (14), the relation between the DC output voltage V_O and DC terms V_G and I_W of the input voltage and the controlling current may be obtained in the form:

$$I_W - G \cdot V_O = G_Z \cdot \frac{V_O \cdot (V_G - V_O) + G \cdot [R_2 \cdot V_G - (R_1 + R_2) \cdot V_O]}{V_G + G \cdot V_O \cdot (R_2 - R_1)}. \tag{19}$$

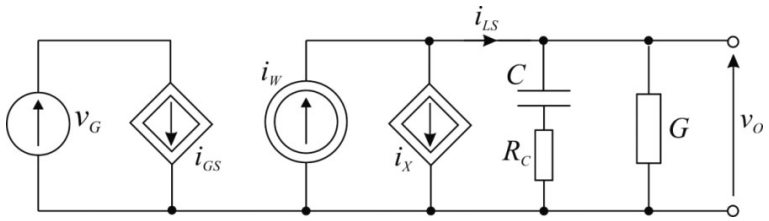

Fig. 4. The averaged DC model of a current-controlled buck converter in CCM

The approximation for $|G(R_2 - R_1)| \ll 1$ leads to the equation:

$$A \cdot V_O^2 - B \cdot V_G \cdot V_O + \frac{I_W}{G_Z} \cdot V_G = 0, \tag{20}$$

where:

$$A = 1 + G \cdot (R_1 + R_2) \tag{21}$$

and

$$B = \frac{G}{G_Z} + G \cdot R_2 + 1. \tag{22}$$

The physically accepted solution of Eq. (20) is:

$$V_O = \frac{V_G \cdot \left(\frac{G}{G_Z} + G \cdot R_2 + 1\right) - \sqrt{V_G^2 \cdot \left(\frac{G}{G_Z} + G \cdot R_2 + 1\right)^2 - 4 \cdot \frac{I_W \cdot V_G}{G_Z} \cdot [1 + G \cdot (R_1 + R_2)]}}{2 \cdot [1 + G \cdot (R_1 + R_2)]}. \tag{23}$$

In the ideal case, $R_1 = R_2 = 0$, we obtain:

$$V_O = \frac{V_G}{2} \cdot \left(\frac{G}{G_Z} + 1\right) - \frac{1}{2} \cdot \sqrt{V_G^2 \cdot \left(\frac{G}{G_Z} + 1\right)^2 - 4 \cdot \frac{I_W \cdot V_G}{G_Z}}. \tag{24}$$

Alternatively, the DC voltage transfer function $M_V = V_O/V_G$ may be obtained from Eq. (20):

$$M_V = \frac{\frac{G}{G_Z} + G \cdot R_2 + 1 - \sqrt{\left(\frac{G}{G_Z} + G \cdot R_2 + 1\right)^2 - \frac{4 \cdot I_W}{G_Z \cdot V_G} \cdot [1 + G \cdot (R_1 + R_2)]}}{2 \cdot [1 + G \cdot (R_1 + R_2)]}. \tag{25}$$

Transfer function M_V for an ideal case have been presented in [30] and the related formula corresponds to (25) for $R_1 = R_2 = 0$. Another possibility is to express M_V as a function of V_O and I_W:

$$M_V = \frac{G_Z \cdot (1 + G \cdot R_2) + G - \frac{I_W}{V_O}}{G_Z \cdot [1 + G \cdot (R_1 + R_2)]}. \tag{26}$$

The additional equation in the DC averaged model is a description of the DC term of input current

$$I_G = \frac{G \cdot V_O^2}{V_G} \cdot (1 + G \cdot R_2). \tag{27}$$

4. Small-signal model

A small-signal model is obtained from the large-signal one by finding the linear equivalent for the nonlinear description of current sources i_X and i_{GS}, namely:

$$i_X = f_1\left(v_O, v_G, i_{LS}\right), \tag{28}$$

$$i_{GS} = f_2\left(v_O, v_G, i_{LS}\right), \tag{29}$$

expressed by Eqs. (14) and (12). The s-domain representation of the small-signal terms of the currents i_X and i_{GS} are:

$$I_x = \frac{\partial f_1}{\partial v_O} \cdot V_o + \frac{\partial f_1}{\partial v_G} \cdot V_g + \frac{\partial f_1}{\partial i_{LS}} \cdot I_l\,, \tag{30}$$

$$I_g = \frac{\partial f_2}{\partial v_O} \cdot V_o + \frac{\partial f_2}{\partial v_G} \cdot V_g + \frac{\partial f_2}{\partial i_{LS}} \cdot I_l\,, \tag{31}$$

where V_o, V_g and I_l are the s-domain representation of small-signal terms of v_O, v_G and i_L.

In the calculations of derivatives given in Eqs. (30) and (31), the approximated form of Eqs. (12) and (14) are used for $|G(R_2 - R_1)| \ll 1$. The resulting expressions for the small-signal quantities are as follows:

$$G_o = \frac{\partial f_1}{\partial v_O} = G_Z \cdot \left[1 - \frac{V_O}{V_G} \cdot (2 + G \cdot (R_1 + R_2))\right], \tag{32}$$

$$G_{mx} = \frac{\partial f_1}{\partial v_G} = G_Z \cdot \frac{V_O^2}{V_G^2} \cdot [1 + G \cdot (R_1 + R_2)], \tag{33}$$

$$K_m = \frac{\partial f_1}{\partial i_L} = G_Z \cdot \left[R_2 - \frac{V_O}{V_G} \cdot (R_1 + R_2)\right], \tag{34}$$

$$G_{mg} = \frac{\partial f_2}{\partial v_O} = \frac{I_L}{V_G} = G \cdot \frac{V_O}{V_G}\,, \tag{35}$$

$$G_{in} = \frac{\partial f_2}{\partial v_G} = -\frac{V_O^2}{V_G^2} \cdot (1 + G \cdot R_2) \cdot G, \tag{36}$$

$$K_g = \frac{\partial f_2}{\partial i_{LS}} = \frac{V_O}{V_G} \cdot (1 + 2 \cdot R_2 \cdot G)\,. \tag{37}$$

A small-signal equivalent circuit of a current-controlled buck converter working in a CCM is shown in Fig. 5. The small-signal term V_o of the output voltage, according to Fig. 5 is:

$$V_o = \frac{\left(I_w - G_{mx} \cdot V_g\right) \cdot Z_c}{1 + K_m + G_o \cdot Z_c}\,, \tag{38}$$

where:

$$Z_c = \frac{s \cdot C \cdot R_C + 1}{s \cdot C \cdot (1 + R_C \cdot G) + G}\,. \tag{39}$$

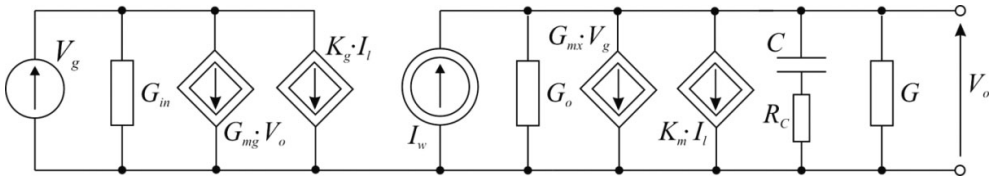

Fig. 5. Small-signal model of a current-controlled buck converter in CCM

Several transmittances may be calculated from the obtained model, such as control-to-output transmittance H_w and input-to-output transmittance H_g. For example:

$$H_w = \left.\frac{V_o}{I_w}\right|_{V_g=0} = \frac{Z_c}{1 + K_m + G_o \cdot Z_c}, \tag{40}$$

By introducing Eqs. (32, 34) and (39) into (40) one obtains an expression for transmittance H_w in the form:

$$H_w = H_{wo} \cdot \frac{1 + s/\omega_z}{1 + s/\omega_p}, \tag{41}$$

where H_{wo} is the low-frequency value of H_w, ω_z and ω_p are the circular frequencies of zero and a pole of the control–to output transmittance.

$$H_{wo} = \frac{1}{G + G_Z \cdot (1 - 2 \cdot M_V) + G \cdot G_Z \cdot R_2 - 2 \cdot G \cdot G_Z \cdot M_V \cdot (R_1 + R_2)}, \tag{42}$$

$$\omega_z = \frac{1}{C \cdot R_C}, \tag{43}$$

$$\omega_p = \frac{G + G_Z \cdot (1 - 2 \cdot M_V) + G \cdot G_Z \cdot R_2 - 2 \cdot G \cdot G_Z \cdot M_V \cdot (R_1 + R_2)}{C_Z + C_Z \cdot G_Z \cdot [R_2 - M_V \cdot (R_1 + R_2)] + [1 - 2 \cdot M_V - G \cdot M_V \cdot (R_1 + R_2)] \cdot G_Z \cdot R_C \cdot C}, \tag{44}$$

where:

$$C_Z = C \cdot (1 + R_C \cdot G). \tag{45}$$

For an ideal converter, $R_1 = R_2 = R_C = 0$, we have:

$$\frac{1}{\omega_z} = 0, \tag{46}$$

$$H_{wo} = \frac{1}{G + G_Z \cdot (1 - 2 \cdot M_V)}, \tag{47}$$

$$\omega_p = \frac{G + G_Z \cdot (1 - 2 \cdot M_V)}{C}. \tag{48}$$

Other small-signal transmittances for a current-controlled buck converter may be obtained in a similar way.

According to Eqs. (47) and (48), the expression for H_{wo} may give undetermined results and ω_P tends to zero, if:

$$M_V \to 0.5 \cdot \left(1 + \frac{G}{G_Z}\right), \tag{49}$$

or, for small G, if:

$$M_V \to 0.5. \tag{50}$$

This observation coincides with the known feature of a current-controlled buck converter, that it may be unstable for a duty ratio (being in an ideal case equal to M_V) approaching 0.5 [5, 6, 13].

5. Simulations and measurements

The verification of the obtained models has been performed by comparison of the results of calculations based on the equations given in Sections 2–4 with full-wave PSpice simulations and measurements in the laboratory model of the converter presented in Fig. 6. The control quantity i_W is obtained in this circuit as:

$$i_W = \frac{v_W}{K \cdot R_F}. \tag{51}$$

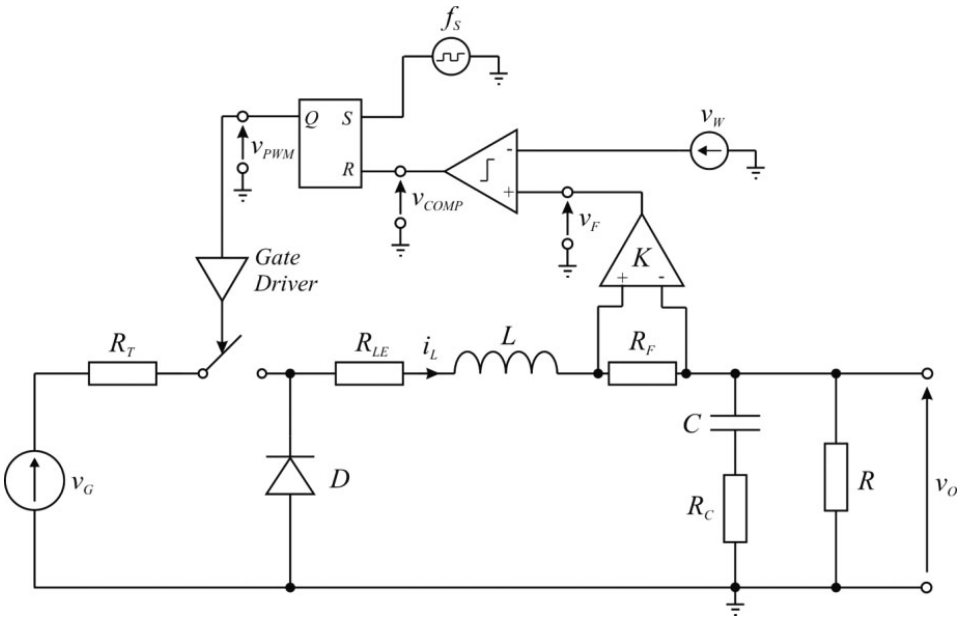

Fig. 6. Power stage of a current-controlled buck converter

Particulars of the measurement circuit are shown in Appendix.

The calculations and measurements have been performed for the following values of converter parameters: input voltage $v_G = 12$ V, switching frequency $f_S = 200$ kHz, load resistance $R = 2.4\ \Omega$, $L = 10\ \mu$H, $R_L = R_{LE} + R_F = 135\ m\Omega$, $C = 470\ \mu$F, $R_C = 76\ m\Omega$, switch: transistor IRFR3806 (described in simulations as resistance $R_T = 40\ m\Omega$ in *ON* subinterval), diode MBRD4040, $R_D = 200\ m\Omega$. Fig. 7 presents the results of time-domain PSpice simulations of the circuit in Fig. 6 for several switching periods in steady-state conditions. The time shift

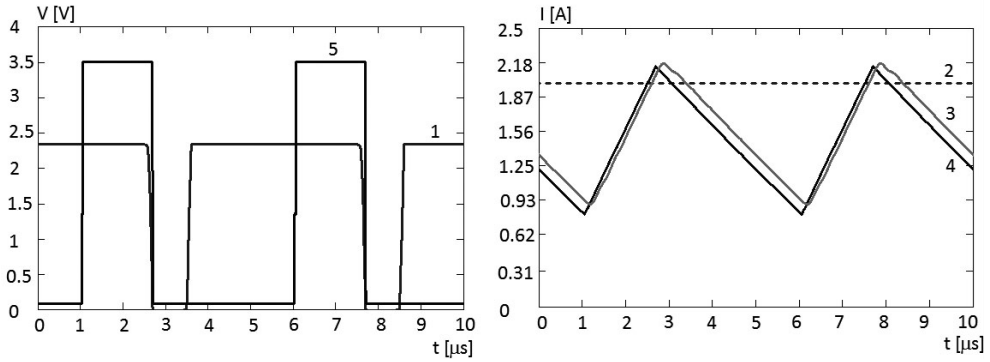

Fig. 7. The PSpice waveforms of the characteristic quantities in converter for constant values $I_W = 2$ A: (1) v_{COMP}, (2) i_W, (3) $v_F/(R_F \cdot K)$, (4) i_L, (5) v_{PWM}

between waveforms of the inductor current i_L and the current corresponding to the voltage v_F is the result of the non-ideality of the amplifier K.

The comparison of the calculation results for the averaged models represented by Figs. 3–5 and Eqs. (14)–(17), (23) and (41)–(45) with the measurements or PSpice for full-wave simulations of the converter are shown in Figs. 8, 9 and 10.

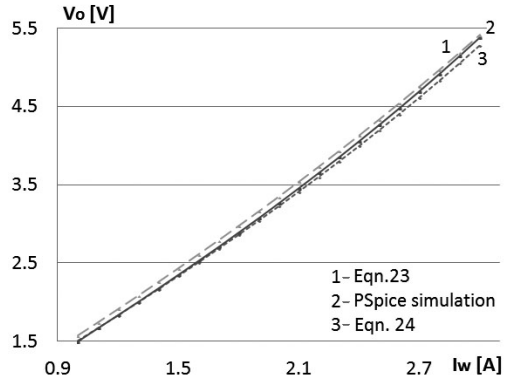

Fig. 8. DC dependencies of the output voltage V_O on the control current I_W

Curves 1 (full wave simulations including real parameters of a comparator and differential amplifier), 2 (measurement) and 3 (full wave simulations with idealized descriptions of the comparator and amplifier) in Figs. 10(a) and (b) are obtained by large signal full-wave PSpice simulations for the circuit in Fig. 6 with the assumed control voltage:

$$v_W(t) = V_W + V_m \cdot \sin(2\pi f t), \tag{52}$$

with $V_W = 2$ V and $V_m = 50$ mV (corresponding to DC component $I_W = 2$ A and the amplitude of the harmonic term $I_{wm} = 50$ mA); curves 4 (a small-signal averaged model with parasitic resistances) and 5 (a small-signal averaged model without parasitic resistances).

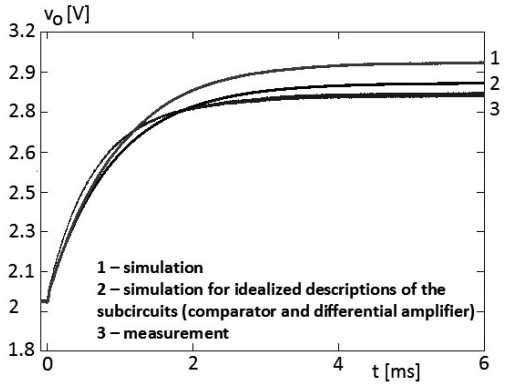

Fig. 9. Time-domain response of the output voltage $V_O(t)$ on the step change of the control current i_W from 1.3 A to 1.8 A

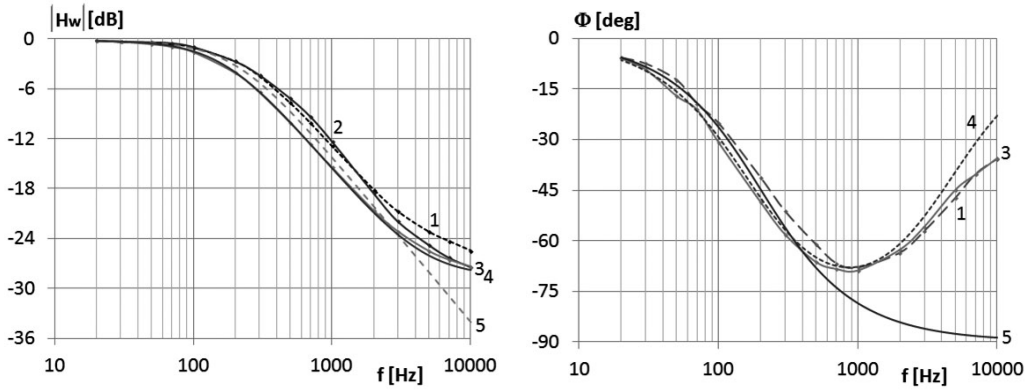

(a) (b)

Fig. 10. Small signal transmittance H_W (see Eq. (40)): (a) magnitude (normalized to 1Ω); (b) phase

6. Conclusions

The averaged models: an AC large signal, DC and AC small signals of a current-controlled non-ideal buck converter in a continuous conduction mode (CCM) are presented and verified by measurements and PSpice simulations. A satisfactory consistency of the calculations based on presented models with the results of measurements and large-signal full-wave PSpice simulations is achieved. The derivation of the model is based on the separation of the variables method and differs from the approach presented usually in the literature, because the multi-loop description of current control is not used. The descriptions of the power stage of a converter in the form of equations and equivalent circuits shown in Sections 2–4 gives a base for the analysis of the full converter (the power stage and a control circuit) treated as a single loop system. One of the interesting features of the presented model, in the small-signal variant, is the observation that the formulas for parameters in the description of the control-to-output transmittance H_w may

give undetermined results in the situation corresponding to duty ratio D_A approaching 0.5 (see Eqs. (47)–(50)). The phenomenon of the current-controlled converter instability at $D_A \to 0.5$ is well known but according to many opinions (for example in [12, 18]) it cannot be explained by the continuous-time models. It seems that our model gives such a possibility.

The proposed approach may be applied to other switch-mode converters as well as to buck converters working in a discontinuous conduction mode (DCM) but the detailed derivations and the resulting equations should be, of course, different.

Appendix

Detailed version of the measurement circuit

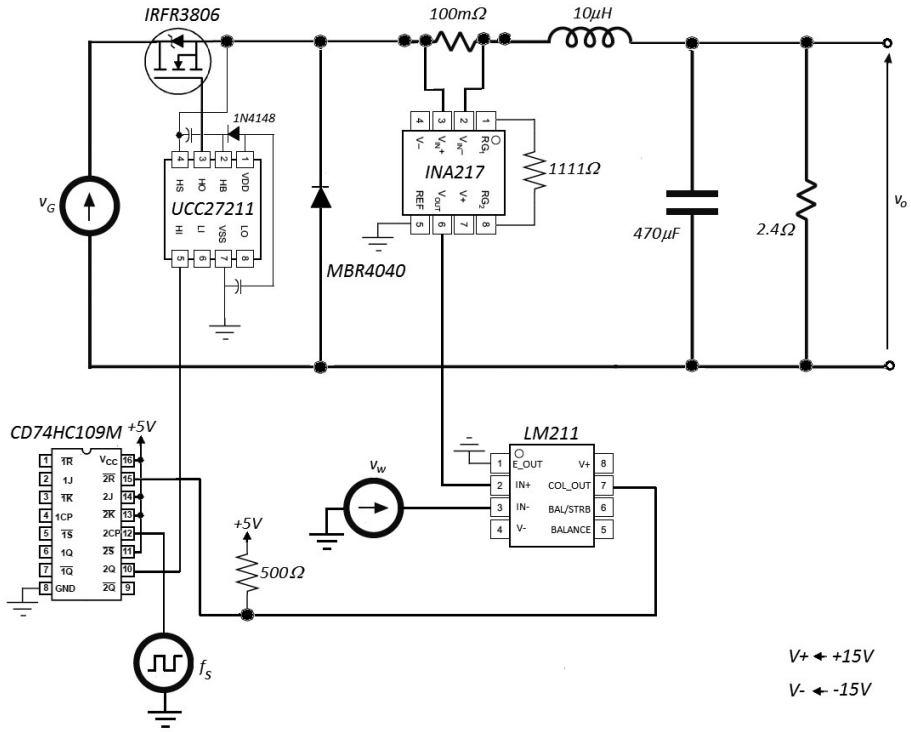

Fig. 11. Particulars of the measurement circuit

References

[1] Erickson R.W., Maksimovic D., *Fundamentals of Power Electronics*, 2-nd Edition, Kluwer (2002).

[2] Kazimierczuk M.K., *Pulse-Width Modulated DC–DC Power Converters*, J. Wiley (2008).

[3] Deisch C.W., *Simple Switching Control Method Changes Power Converter into a Current Source*, IEEE PESC, Record, pp. 300–306 (1978).

[4] Capel A., Ferrante G., O'Sullivan D., Weinberg A., *Application of the Injected Current Model for the Dynamic Analysis of Switching Regulators with the New Concept of LC^3 Modulator*, IEEE PESC, Record, pp. 135–147 (1978).

[5] Hsu S.-P., Brown A., Rensink L., Middlebrook R.D., *Modelling and Analysis of Switching Dc-to-Dc Converters in Constant-Frequency Current-Programmed Mode*, IEEE PESC, pp. 284–301 (1979).

[6] Middlebrook, R.D., *Topics in Multiple-Loop Regulators and Current Mode Programming*, IEEE Transactions on Power Electronics, vol. PE-2, no. 2, pp. 109–124 (1987).

[7] Middlebrook R.D., *Modeling Current-Programmed Buck and Boost Regulators*, IEEE Transactions on Power Electronics, vol. 4, no. 1, pp. 36–52 (1989).

[8] Ridley R.B., Cho B.H., Lee F.C.Y., *Analysis and Interpretation of Loop Gains of Multiloop-Controlled Switching Regulators*, IEEE Transactions on Power Electronics, vol. 3, no. 4, pp. 489–498 (1988).

[9] Vorperian V., *Simplified Analysis of PWM Converters using Model of PWM Switch, Part I: Continuous Conduction Mode*, IEEE Transactions on Aerospace and Electronic Systems, vol. 26, no. 3, pp. 490–496 (1990).

[10] Vorperian V., *Simplified analysis of PWM converters using the model of the PWM switch, Part II: Discontinuous Conduction Mode*, IEEE Transactions on Aerospace and Electronic Systems, vol. 26, no. 3, pp. 497–505 (1990).

[11] Ben-Yaakov S., *Average simulation of PWM converters by direct implementation of behavioural relationships*, International Journal of Electronics, vol. 77, no. 5, pp. 731–746 (1994).

[12] Ridley R.B., *A New, Continuous-Time Model For Current-Mode Control*, IEEE Transactions on Power Electronics, vol. 6, no. 2, pp. 271–280 (1991).

[13] Ridley R.B., *An Accurate and Practical Small-Signal Model for Current-Mode Control*, Ridley Engineering, Inc., pp. 1–22 (1999).

[14] Li J., Lee F.C., *New Modeling Approach and Equivalent Circuit Representation for Current-Mode Control*, IEEE Transactions on Power Electronics, vol. 25, no. 5, pp. 1218–1230 (2010).

[15] Yu F., Lee F.C., Mattavelli P., *A Small Signal Model for Average Current Mode Control Based On Describing Function Approach*, IEEE Energy Conversion Congress and Exposition, pp. 405–412 (2011).

[16] Yan Y., Lee F.C., Mattavelli P., *Unified Three-Terminal Switch Model for Current Mode Controls*, IEEE Transactions on Power Electronics, vol. 27, no. 9, pp. 4060–4070 (2012).

[17] Yan Y., Lee F.C., Mattavelli P., *Dynamic performance comparison of Current Mode Control Schemes for Point-of-Load Buck Converter Application*, IEEE APEC, pp. 2484–2491 (2012).

[18] Yan Y., Lee F.C., Mattavelli P., *I2 Average Current Mode Control for Switching Converters*, IEEE Transactions on Power Electronics, vol. 29, no. 4, pp. 2027–2036 (2014).

[19] Saini D., Reatti A., Kazimierczuk M., *Average current-mode control of buck dc-dc converter with reduced control voltage ripple*, 42nd Annual Conference of the IEEE Industrial Electronics Society – IECON, pp. 3270–3275 (2016).

[20] Saini D., Kazimierczuk M., *Audio-susceptibility of inner loop of true-average current-mode controlled buck dc-dc converter*, IEEE 60th International Midwest Symposium on Circuits and Systems (MWSCAS), pp.460–463 (2017).

[21] Suntio T., *On Dynamic Modeling of PCM-Controlled Converters – Buck Converter as an Example*, IEEE Transactions on Power Electronics, vol. 33, iss. 6, pp. 5502–5518 (2018).

[22] Zhu D., Wang Y., Duan J., Wang R., *Modeling and Bifurcation Analysis of Buck Converters Under Peak Current-Mode Control*, Chinese Automation Congress (CAC), pp. 2563–2568 (2018).

[23] Chiu Y.T., Liu Y.H., Hung C.C., *A high-performance current-mode DC-DC buck converter with adaptive clock control technique*, 2018 International Symposium on VLSI Design, Automation and Test (VLSI-DAT) (2018), DOI: 10.1109/VLSI-DAT.2018.8373259.

[24] Chen J.J., Hwang Y.S., Hwang B.H., Jhang Y.C., Ku Y.T., *A dual-mode fast-transient average-current-mode buck converter without slope-compensation*, 7th International Symposium on Next Generation Electronics (ISNE) (2018), DOI: 10.1109/ISNE.2018.8394680.

[25] Kang J.G., Park J., Jeong M.G., Yoo C., *A Time-Domain-Controlled Current-Mode Buck Converter With Wide Output Voltage Range*, IEEE Journal of Solid-State Circuits, vol. 54, iss., (2019), DOI: 10.1109/JSSC.2018.2884912.

[26] Kajiwara K., Yamasaki K., Matsui N., Kurokawa F., *Stability of Digital Hysteresis Current Mode Buck Converter for DC Distribution System*, 7th International Conference on Renewable Energy Research and Applications (ICRERA 2018), pp. 1321–1324 (2018).

[27] Jeong M.G., Kang J.G., Park J., Yoo C., *A Current-Mode Hysteretic Buck Converter with Multiple-Reset RC-Based Inductor Current Sensor*, IEEE Transactions on Industrial Electronics (2019), DOI: 10.1109/TIE.2018.2889613.

[28] Janke W., *Averaged models of pulse-modulated DC-DC power converters. Part I. Discussion of standard methods*, Archives of Electrical Engineering, vol. 61, no. 4, pp. 609–631 (2012).

[29] Janke W., *Averaged Models of Pulse-Modulated DC-DC Converters, Part II. Models Based on the Separation of Variables*, Archives of Electrical Engineering, vol. 61, no. 4, pp. 633–654 (2012).

[30] Janke W., Kraśniewski J., *Averaged model of pulse-type current-programmed Buck DC–DC converter*, Electrical Review (in Polish), no. 8, pp. 120–123 (2017).